

# 2D Molecular Superconductor to Insulator Transition in the $\beta''$ - (BEDT-TTF)<sub>2</sub>[(H<sub>2</sub>O)(NH<sub>4</sub>)<sub>2</sub>M(C<sub>2</sub>O<sub>4</sub>)<sub>3</sub>].18-crown-6 series (M = Rh, Cr, Ru, Ir)

Alexander L. Morritt,<sup>†</sup> Jordan R. Lopez,<sup>†</sup> Toby J. Blundell,<sup>†</sup> Enric Canadell,<sup>‡</sup> Hiroki Akutsu,<sup>§</sup>  
Yasuhiro Nakazawa,<sup>§</sup> Shusaku Imajo,<sup>||</sup> Lee Martin,<sup>†\*</sup>

<sup>†</sup>School of Science and Technology, Nottingham Trent University, Clifton Lane, Nottingham, NG11 8NS,  
United Kingdom

<sup>‡</sup>Institut de Ciència de Materials de Barcelona (ICMAB-CSIC), Campus de la UAB, 08193 Bellaterra, Spain

<sup>§</sup>Department of Chemistry, Graduate School of Science, Osaka University, 1-1 Machikaneyama, Toyonaka,  
Osaka 560-0043, Japan.

<sup>||</sup>Institute for Solid State Physics, University of Tokyo, Kashiwa 277-8581, Japan

**ABSTRACT:** The series of salts  $\beta''$ -(BEDT-TTF)<sub>2</sub>[(H<sub>2</sub>O)(NH<sub>4</sub>)<sub>2</sub>M(C<sub>2</sub>O<sub>4</sub>)<sub>3</sub>].18-crown-6 show ambient-pressure superconductivity when M = Cr or Rh. Evidence indicates that the previously reported Cr and Rh salts show a bulk Berezinski-Kosterlitz-Thouless superconducting transition. The isostructural ruthenium and iridium salts are reported here. The Ir salt represents the first radical-cation salt to contain a 5d tris(oxalato)metallate anion. Both the Ru and Ir salts do not show superconductivity but instead undergo a broad chemically-induced metal-to-insulator transition at 155 K for ruthenium and at 100 K for iridium. The *c* axes of the Ru and Ir salts are much shorter than those of the Rh and Cr salts. Thus the more stable metallic state of the Cr and Rh salts is associated with the more strongly 2D electronic systems. The different low-temperature behaviour of the Ru and Ir salts, which exhibit a smaller interlayer spacing, could originate from a structural change in the anionic layer which thus can be easily transmitted to the donor layers and generate a localized state. However another possibility is that it originates from Berezinski-Kosterlitz-Thouless effects.

## INTRODUCTION

Radical-cation salts of BEDT-TTF with tris(oxalato)metallate anions have produced a multitude of multifunctional materials over the past 25 years.<sup>1</sup> These salts have combined conductivity with paramagnetism,<sup>2</sup> ferromagnetism,<sup>3</sup> or anti-ferromagnetism<sup>4</sup> through making slight modifications to the lattice by changing the metal of the trisoxalate, the cation, or the guest solvent molecule.<sup>1</sup> The general formula for most of these radical-cation salts is (BEDT-TTF)<sub>x</sub>[(cation)M(C<sub>2</sub>O<sub>4</sub>)<sub>3</sub>].guest (*x* = 3 or 4).<sup>1</sup> The BEDT-TTF donors and the tris(oxalato)metallate anions form separate layers. The anion layers are formed of a honeycomb of tris(oxalato)metallate anions and cations with guest solvent molecules situated within the hexagonal cavities created by the honeycomb arrangement. The packing arrangement of the donor layer, and therefore the conductivity of the material, is dictated by the size of the hexagonal cavities and the size, shape, and orientation of the guest solvent molecule within it. Small cations (e.g. Li<sup>+</sup>, Na<sup>+</sup>) and guest molecules (e.g. nitromethane, acetonitrile, ethanol, DCM, DMF, acetonitrile) produce semi-conducting salts where *x* = 3.<sup>5</sup> Larger cations (e.g. NH<sub>4</sub><sup>+</sup>, K<sup>+</sup>) and guest molecules (e.g. benzonitrile, nitrobenzene, halobenzenes) produce salts where *x* = 4 that can show superconductivity.<sup>2,6</sup> Increasing the size of the guest molecule further (e.g. acetophenone, sec-phenethyl alcohol) means that the guest molecule does not fit within the hexagonal cavity and part of the guest molecule projects out of one side of the anion layer and leads to a different BEDT-TTF packing motif being present on each side of the anion layer, e.g. both  $\alpha$  and  $\beta''$ ,<sup>7</sup> or  $\alpha$  and  $\kappa$ .<sup>8</sup>

Owing to its affinity for NH<sub>4</sub><sup>+</sup> and K<sup>+</sup> cations, 18-crown-6 is used in the synthesis of these radical-cation salts. It has been shown that the crown ether molecule can also be included in the crystal structure,<sup>9</sup> and this has produced a salt which is both metallic and a proton conductor.<sup>10</sup> The crown ether is also included in the lattice of the title material,  $\beta''$ -(BEDT-TTF)<sub>2</sub>[(H<sub>2</sub>O)(NH<sub>4</sub>)<sub>2</sub>M(C<sub>2</sub>O<sub>4</sub>)<sub>3</sub>].18-crown-6, which represents only the second family of BEDT-TTF-tris(oxalato)metallate radical-cation salts to exhibit superconductivity.<sup>11</sup> The distance between neighbouring conducting

layers in this salt is the widest found in a radical-cation salt having just the one BEDT-TTF packing type ( $\beta''$ ).<sup>11</sup> We have previously reported that when  $M = \text{Cr}$  or  $\text{Rh}$  evidence indicates that a bulk Berezinski-Kosterlitz-Thouless superconducting transition is observed and there is a broad transition from  $T_c$  to  $T_{\text{zero}}$ .<sup>12</sup> We report here the isostructural  $\beta''$ -(BEDT-TTF)<sub>2</sub>[(H<sub>2</sub>O)(NH<sub>4</sub>)<sub>2</sub>M(C<sub>2</sub>O<sub>4</sub>)<sub>3</sub>].18-crown-6 salts where  $M = \text{ruthenium}$  or  $\text{iridium}$ . The Ir salt represents the first radical-cation salt to contain a 5d tris(oxalato)metallate anion. Both the Ru and Ir salts do not show superconductivity but instead undergo a broad chemically-induced metal-to-insulator transition at 155 K for ruthenium and at 100 K for iridium.

## RESULTS AND DISCUSSION

All four salts crystallise in triclinic  $P-1$  space group with a formula of  $\beta''$ -(BEDT-TTF)<sub>2</sub>[(H<sub>2</sub>O)(NH<sub>4</sub>)<sub>2</sub>M(C<sub>2</sub>O<sub>4</sub>)<sub>3</sub>].18-crown-6 (where  $M = \text{Cr, Rh, Ru, Ir}$ ). The **Ru** and **Ir** salts are isostructural with the previously published **Cr** and **Rh** salts.<sup>11</sup> The structure consists of  $\beta''$  BEDT-TTF layers and H<sub>2</sub>O/NH<sub>4</sub><sup>+</sup>/18-crown-6 layers which are segregated by layers of NH<sub>4</sub><sup>+</sup>/tris(oxalato)metallate (Fig. 1). Each tris(oxalato)metallate layer consists of only a single enantiomer with the next tris(oxalato)metallate layer containing the opposing enantiomer. Table 1 compares the unit cell dimensions of all four salts at 110K. Of note is that the  $c$  axes of the **Ru** and **Ir** salts are much shorter than those observed previously in the superconducting **Cr** and **Rh** salts.<sup>11</sup>

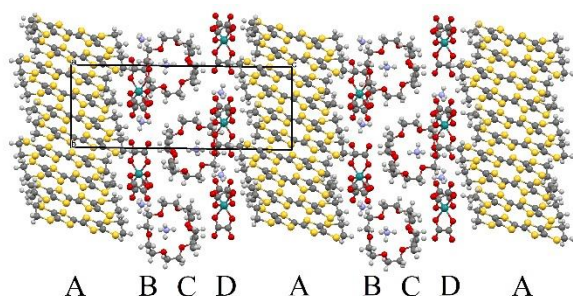


**Fig. 1** Crystal structure of  $\beta''$ -(BEDT-TTF)<sub>2</sub>[(H<sub>2</sub>O)(NH<sub>4</sub>)<sub>2</sub>M(C<sub>2</sub>O<sub>4</sub>)<sub>3</sub>].18-crown-6 projected along the  $b$  axis. The layered packing can be seen with donor layers (A) and crown ether layers (C) sandwiched between enantiopure layers of either  $\Lambda$  or  $\Delta$  tris(oxalato)metallate (B and D). This gives a lattice with ABCDABCDA arrangement of layers.

	$a / \text{\AA}$	$b / \text{\AA}$	$c / \text{\AA}$	$\alpha / ^\circ$	$\beta / ^\circ$	$\gamma / ^\circ$	$V / \text{\AA}^3$
<b>Cr</b>	10.2565(6)	11.1039(7)	27.3786(15)	86.474(6)	82.734(6)	64.165(5)	2783.8(3)
<b>Rh</b>	10.2970(5)	11.2532(4)	27.4339(11)	86.383(3)	82.411(4)	64.325(4)	2839.9(2)
<b>Ru</b>	10.2959(2)	11.1722(3)	27.1422(5)	86.329(6)	82.859(6)	64.347(5)	2792.35(15)
<b>Ir</b>	10.3115(3)	11.1855(4)	27.1250(7)	86.213(6)	82.827(6)	64.215(5)	2794.78(18)

**Table 1** Unit cell dimensions of the  $\beta''$ -(BEDT-TTF)<sub>2</sub>[(H<sub>2</sub>O)(NH<sub>4</sub>)<sub>2</sub>M(C<sub>2</sub>O<sub>4</sub>)<sub>3</sub>].18-crown-6 salts at 110K.

The anion layer is the same as that found in the  $\beta''$ -(BEDT-TTF)<sub>4</sub>[(A)M(C<sub>2</sub>O<sub>4</sub>)<sub>3</sub>].Guest<sup>2</sup> salts with a hexagonal cavity built from cations and tris(oxalato)metallates (Fig. 2). The guest in this case is an 18-crown-6 ether (layer C) which projects into the hexagon in one or other of the neighbouring layers (layer B or D) (Figs. 1 and 3).

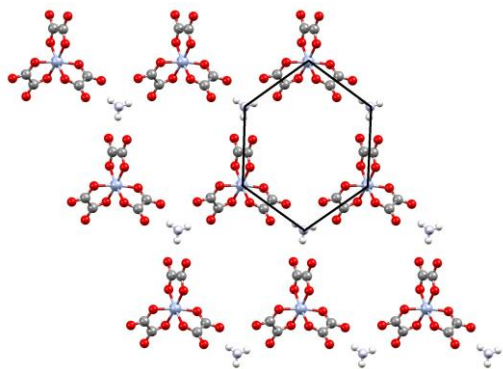


**Fig. 2** Anion layer of  $\beta''$ -(BEDT-TTF)<sub>2</sub>[(H<sub>2</sub>O)(NH<sub>4</sub>)<sub>2</sub>M(C<sub>2</sub>O<sub>4</sub>)<sub>3</sub>].18-crown-6 projected along the  $c$  axis. The black line indicates a hexagonal cavity formed by three tris(oxalato)metallate anions with three ammonium cations.

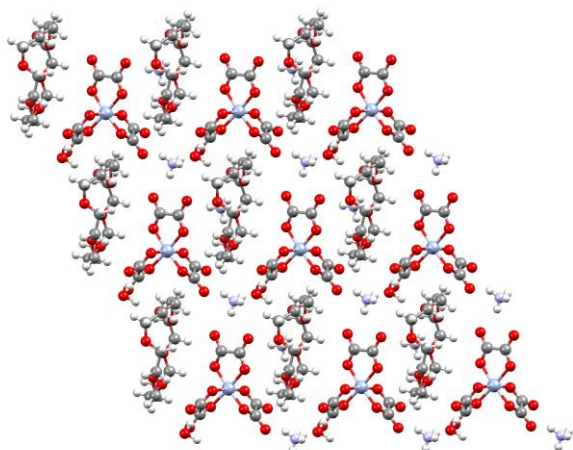
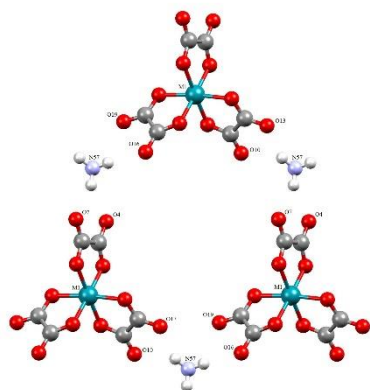


**Fig. 3** Anion layer of  $\beta''$ -(BEDT-TTF)<sub>2</sub>[(H<sub>2</sub>O)(NH<sub>4</sub>)<sub>2</sub>M(C<sub>2</sub>O<sub>4</sub>)<sub>3</sub>].18-crown-6 showing the neighbouring 18-crown-6 molecules which are located in the hexagonal cavities.

Table 2 shows the hexagonal cavity dimensions for all four salts. We previously reported that the **Cr** salt has a hexagonal cavity similar in dimensions to superconductor  $\beta''$ -(BEDT-TTF)<sub>4</sub>[(H<sub>3</sub>O)Cr(C<sub>2</sub>O<sub>4</sub>)<sub>3</sub>].benzotrifluoride.<sup>11</sup> In the  $\beta''$ -(BEDT-TTF)<sub>2</sub>[(H<sub>2</sub>O)(NH<sub>4</sub>)<sub>2</sub>M(C<sub>2</sub>O<sub>4</sub>)<sub>3</sub>].18-crown-6 series (M = **Cr**, **Rh**, **Ru**, **Ir**), the **Cr** hexagonal cavity is the smallest and the **Rh** the largest. **Ru** and **Ir** are intermediate, with both being very similar in size, and only slightly smaller than **Rh**. Previous work<sup>6</sup> reported that the hexagonal cavity dimensions are dependent upon the size of the metal<sup>3+</sup> and the oxygen...cation distances rather than the size of the solvent cited within the hexagonal cavity. The **Rh** salt has some of the longest distances from outer oxalate oxygens to ammonium cations (3.083(5) Å) compared to **Ru** (3.047(3) Å), **Ir** (3.037(7) Å) and **Cr** (3.039(7) Å).



Distances / Å	<b>Rh</b>	<b>Cr</b>	<b>Ru</b>	<b>Ir</b>
HEXAGON SIDES e.g. M1 to N57	6.443(3) 6.372(3) 6.338(3)	6.353(5) 6.327(5) 6.280(7)	6.398(2) 6.365(2) 6.319(2)	6.400(5) 6.367(5) 6.323(5)
HEIGHT e.g. top M1 to bottom N57	13.861(3) 12.358(3) 11.931(3)	13.655(5) 12.284(5) 11.841(5)	13.768(2) 12.360(2) 11.880(2)	13.764(5) 12.358(5) 11.910(5)
WIDTH 3 possible M1 to M1 or N57 to N57	11.5002(7) 11.2532(4) 10.2970(5)	11.3680(8) 11.1039(7) 10.2565(6)	11.4555(7) 11.1722(3) 10.2959(2)	11.4498(7) 11.1856(4) 10.3115(3)
Oxalate O4-cation N57	2.951(4)	2.924(6)	2.916(3)	2.916(6)
Oxalate O7-cation N57	3.034(4)	3.013(7)	2.991(3)	3.009(7)
Oxalate O10-cation N57	2.839(4)	2.834(6)	2.832(3)	2.816(6)
Oxalate O13-cation N57	3.057(4)	3.026(6)	3.004(3)	3.034(7)
Oxalate O16-cation N57	2.903(4)	2.913(6)	2.884(3)	2.910(7)
Oxalate O19-cation N57	3.083(5)	3.039(7)	3.047(3)	3.037(7)

**Table 2** Selected distances and angles for the anion layer of the  $\beta''$ -(BEDT-TTF)<sub>2</sub>[(H<sub>2</sub>O)(NH<sub>4</sub>)<sub>2</sub>M(C<sub>2</sub>O<sub>4</sub>)<sub>3</sub>].18-crown-6 salts.

The  $\beta''$  donor packing arrangement in **Ru** and **Ir** is isostructural with the previously reported **Cr** and **Rh** salts.<sup>11</sup> The two independent donors adopt an AABBAABBAA arrangement within each donor stack (Fig. 4). At 110K the terminal ethylene at one end of donor A is disordered. Table 3 lists the short sulphur-sulphur contacts in each salt, all of which are ‘side-to-side’ between donors in neighbouring stacks. Using the equation reported by Guionneau *et al.*<sup>13</sup> (Table 4) we estimate a charge of 0.5<sup>+</sup> for each donor which is in agreement with  $\beta''$ -(BEDT-TTF<sup>0.5+</sup>)<sub>2</sub>[(H<sub>2</sub>O)(NH<sub>4</sub><sup>+</sup>)<sub>2</sub>M<sup>3+</sup>(C<sub>2</sub>O<sub>4</sub><sup>2-</sup>)<sub>3</sub>].18-crown-6.

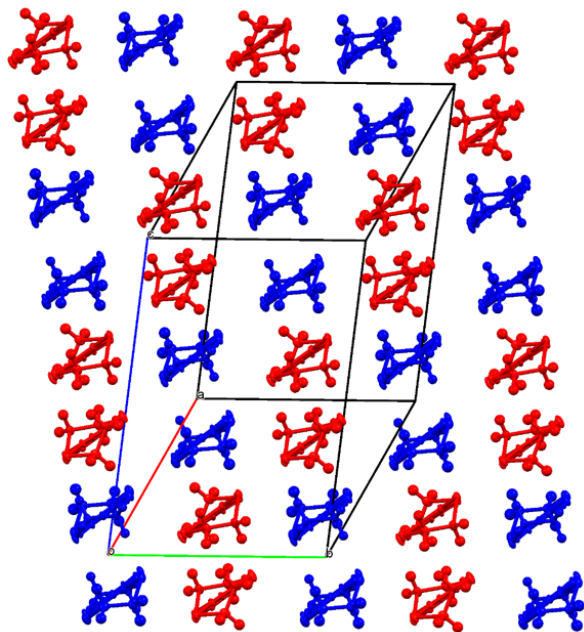
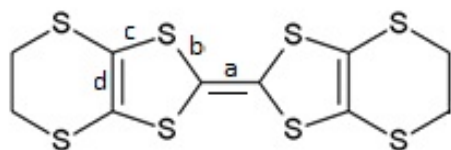


**Fig. 4** BEDT-TTF layer of  $\beta''$ -(BEDT-TTF)<sub>2</sub>[(H<sub>2</sub>O)(NH<sub>4</sub>)<sub>2</sub>M(C<sub>2</sub>O<sub>4</sub>)<sub>3</sub>].18-crown-6. BEDT-TTF molecules are shown end on with molecule A in red and B in blue.

Side-to-side contact/Å	Rh	Cr	Ru	Ir
S32...S50	3.2782 (13)	3.2456(18)	3.2838 (9)	3.3014 (18)
S30...S50	3.3273 (13)	3.2836(18)	3.3058 (9)	3.3172 (18)
S46...S53	3.3527 (12)	3.3326(17)	3.3490 (9)	3.3593 (17)
S46...S55	3.4873 (12)	3.4533(17)	3.4665 (9)	3.4734 (16)
S25...S43	3.5267 (13)	3.5213(18)	3.5315 (9)	3.5299 (18)
S20...S35	3.5712 (12)	3.5397(17)	3.5770 (9)	3.5831 (17)
S25...S38	3.5661 (13)	3.5500(19)	3.5450 (9)	3.5363 (17)

**Table 3** S...S contacts at 110K for the  $\beta''$ -(BEDT-TTF)<sub>2</sub>[(H<sub>2</sub>O)(NH<sub>4</sub>)<sub>2</sub>M(C<sub>2</sub>O<sub>4</sub>)<sub>3</sub>].18-crown-6 salts.



	a / Å	b / Å	c / Å	d / Å	$\delta$	Q
<b>Cr A</b>	1.370	1.740	1.757	1.349	0.778	0.54+
<b>Cr B</b>	1.370	1.744	1.756	1.346	0.784	0.50+
<b>Rh A</b>	1.371	1.749	1.758	1.366	0.770	0.60+
<b>Rh B</b>	1.375	1.752	1.758	1.361	0.773	0.58+
<b>Ru A</b>	1.369	1.738	1.751	1.356	0.764	0.64+
<b>Ru B</b>	1.372	1.741	1.753	1.354	0.768	0.62+
<b>Ir A</b>	1.374	1.739	1.752	1.350	0.767	0.62+
<b>Ir B</b>	1.378	1.743	1.754	1.352	0.767	0.62+

**Table 4** Average bond lengths in BEDT-TTF molecules of the  $\beta''$ -(BEDT-TTF)<sub>2</sub>[(H<sub>2</sub>O)(NH<sub>4</sub>)<sub>2</sub>M(C<sub>2</sub>O<sub>4</sub>)<sub>3</sub>].18-crown-6 salts and approximation of charge on the molecules.  $\delta = (b+c)-(a+d)$ ,  $Q = 6.347-7.463\delta$ .<sup>13</sup>

## TRANSPORT MEASUREMENTS

The previously reported **Rh** salt<sup>11</sup> has a superconducting  $T_c$  of 2.7 K and shows a broad transition which does not reach zero resistivity. The isostructural **Cr** salt<sup>11</sup> has a superconducting  $T_c$  of ~4.0-4.9 K and a broad transition to zero resistivity below 1.8 K. In contrast the isostructural **Ru** and **Ir** salts do not show superconductivity but instead undergo a broad chemically-induced metal-to-insulator transition at 155 K for **Ru** and at 100 K for **Ir** (Fig. 5 and 6).

This is a remarkable difference considering the small differences between these four isomorphous salts. The most notable difference between these salts is in their  $c$  axis length (Table 1) which is 0.055 Å longer in **Rh** compared to **Cr**. Therefore, **Rh** has a bigger distance between conducting layers and is more two-dimensional in nature than **Cr**. We previously reported that we believe the strong 2D nature of the **Rh** and **Cr** salts makes the superconducting transition a Berezinski-Kosterlitz-Thouless (BKT) transition.<sup>11</sup> Zero resistivity is not observed for the **Rh** salt at the lowest temperature of measurement (0.6K) but the data suggests that a perfect BKT transition may be possible at 0K. The **Cr** salt differs in that it shows zero resistivity at a finite temperature (1.8K) which suggests that a perfect 2D nature would be expected in a salt having an insulating layer length intermediate between those of the **Cr** and **Rh** salts. The  $c$  axes of the metal-insulator **Ru** (27.1422(5) Å) and **Ir** (27.1250(7) Å) salts are much shorter than those of the **Cr** (27.3786(15) Å) and **Rh** salt (27.4339(11) Å).

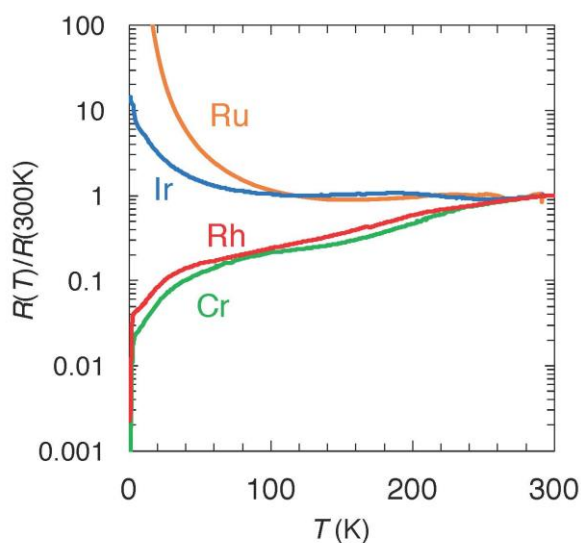


**Fig. 5** Temperature dependence of resistance for **Rh**, **Cr**, **Ru** and **Ir**. The onset of superconductivity is observed at between 4.0 and 4.9K ( $T_{zero} \sim 1.8$ K) for **Cr** and at 2.7K for **Rh**. Metal-Insulator transitions occur at 155 K for **Ru** and at 100 K for **Ir**.

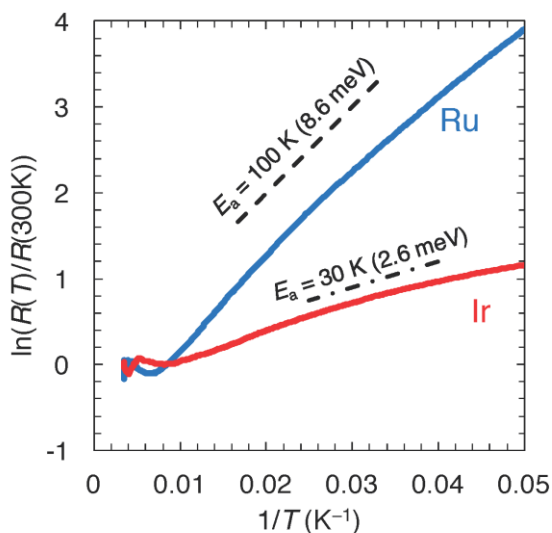


**Fig. 6** Arrhenius plots for **Ru** and **Ir**.

Table 5 shows the three shortest metal-to-metal distances which represent the widths of the insulating layer. As expected from the *c* axis values the width of the insulating layers decreases in the order **Rh** > **Cr** >> **Ru** > **Ir**, with superconducting **Rh** (12.1489(8)-12.3922(7) Å) and **Cr** (12.1459(19)-12.3260(18) Å) having longer M...M distances compared to metal-insulator **Ru** (12.1265(8)-12.2716(6) Å) and **Ir** (12.0889(9)-12.2516(6) Å). Since the direction of the *c* axis corresponds to the interlayer direction, the difference of the electronic states may be expected to originate from dimensionality, *i.e.* interlayer interaction.

Distances / Å	<b>Rh</b>	<b>Cr</b>	<b>Ru</b>	<b>Ir</b>
THREE CLOSEST DISTANCES BETWEEN METAL OF THE TRISOXALATE ON ONE SIDE OF INSULATING LAYER TO METAL ON THE OTHER SIDE	12.1489 (8) 12.2419 (7) 12.3922 (7)	12.1459 (19) 12.1925 (18) 12.3260 (18)	12.1265 (8) 12.1327 (9) 12.2716 (6)	12.0889 (9) 12.1079 (8) 12.2516 (6)

**Table 5** Width of anion layer of the  $\beta''$ -(BEDT-TTF)<sub>2</sub>[(H<sub>2</sub>O)(NH<sub>4</sub>)<sub>2</sub>M(C<sub>2</sub>O<sub>4</sub>)<sub>3</sub>].18-crown-6 salts.

The separation of the donor layers is very large in these salts. Consequently, these systems rank among the better 2D metals known so far. Since the direction of the *c* axis corresponds to the interlayer direction, the two superconducting salts (**Rh**, **Cr**) should have better two-dimensionality compared with the two metal-insulating salts (**Ru**, **Ir**). The change from metal to semiconductor regime in the latter can have several origins: (i) a Peierls transition, (ii) an electron localization due to disorder, (iii) an electronic localization induced by some structural modification occurring in the anionic layer, and (iv) Berezinski-Kosterlitz-Thouless effects. The very broad nature of the transition rules out a Peierls transition. Moreover, the observed SdH oscillation of the **Cr** salt<sup>11</sup> indicates the existence of a two-dimensional Fermi surface whose cross-sectional area is almost equivalent to that of the other  $\beta''$ -type salts.<sup>7</sup> The likeliness of the other three possibilities is discussed in the next section.

## ELECTRONIC STRUCTURE

The donor layers of the  $\beta''$ -(BEDT-TTF)<sub>2</sub>[(H<sub>2</sub>O)(NH<sub>4</sub>)<sub>2</sub>M(C<sub>2</sub>O<sub>4</sub>)<sub>3</sub>].18-crown-6 (M = **Rh**, **Cr**, **Ru**, **Ir**) salts contain two symmetry nonequivalent donors (A and B) and eight different donor...donor interactions labeled I to VIII in Fig. 7. As for any  $\beta''$  salt there are three different types of interactions:<sup>14</sup> (a) along the stacks (I to III in Fig. 7), (b) lateral  $\pi$ -type interactions (IV to VI), and (c) along the step-chains (VII and VIII). The strength of the different HOMO...HOMO intermolecular interactions can be assessed from the so-called  $|\beta_{\text{HOMO-HOMO}}|$  interaction energies.<sup>15</sup> Those calculated for the four salts **Rh**, **Cr**, **Ru**, **Ir** are reported in Table 6. As usual, the HOMO...HOMO interactions along the step-chains are the stronger ones and those along the lateral  $\pi$ -type interactions are still very sizable (*i.e.*, around 60% of those along the step-chains). In contrast with other  $\beta''$  salts of BEDT-TTF and similar anionic layers,<sup>16,17</sup> the interactions along the stacks are clearly weaker. In terms of these HOMO...HOMO interactions the present salts are quite similar to the  $\beta''$ -type molecular superconductor  $\beta''$ -(BEDT-TTF)<sub>4</sub>K<sub>x</sub>(H<sub>3</sub>O)<sub>1-x</sub>[Ru(C<sub>2</sub>O<sub>4</sub>)<sub>3</sub>]C<sub>6</sub>H<sub>5</sub>Br (*x*~0.8).<sup>18</sup> As for this salt the HOMO energies of the two different donors in the four new salts are very similar, differing by only ~0.01 eV. Because of this fact, and since both the interactions along the step-chains and the  $\pi$ -type interactions are substantial, these salts should be two-dimensional conductors.

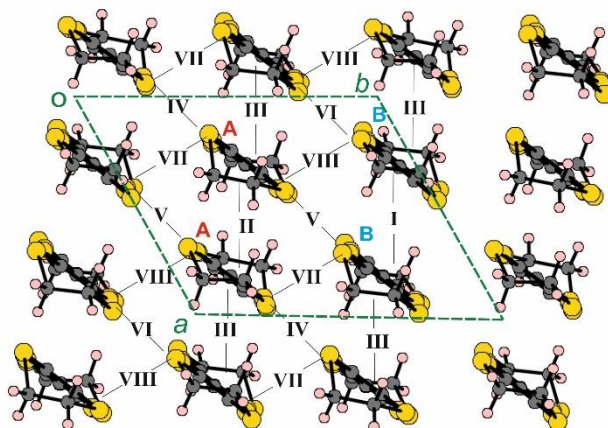


**Fig. 7** Donor layer with the different donors and intermolecular interactions labeled.

Interaction	Interaction	Rh	Cr	Ru	Ir
I	(B-B)	0.0877	0.1003	0.0911	0.0968
II	(A-A)	0.0392	0.0465	0.0252	0.0235
III	(A-B)	0.1461	0.1569	0.1373	0.1385
IV	(A-A)	0.1641	0.1743	0.1657	0.1598
V	(A-B)	0.1588	0.1670	0.1616	0.1593
VI	(B-B)	0.1129	0.1177	0.1140	0.1113
VII	(A-B)	0.2555	0.2640	0.2628	0.2676
VIII	(A-B)	0.2403	0.2477	0.2484	0.2496

**Table 6**  $|\beta_{\text{HOMO-HOMO}}|$  interaction energies (eV) for the different donor...donor interactions in the  $\beta''$ -(BEDT-TTF)<sub>2</sub>[(H<sub>2</sub>O)(NH<sub>4</sub>)<sub>2</sub>M(C<sub>2</sub>O<sub>4</sub>)<sub>3</sub>]-18-crown-6 salts.

The calculated band structures for the **Rh** (room temperature metal and superconductor at low temperature) and **Ru** (room temperature metal but semiconducting at low temperature) salts are reported in Figures 8a and 9a, respectively. Those for the **Cr** and **Ir** salts are reported in the Supplementary information (Figs. S1a and S2a, respectively). All these band structures are very similar. According to the stoichiometry there must be two holes within the four HOMO bands. Since the two upper bands of all the salts overlap they must be both partially filled and the salts should exhibit a metallic behavior. This is in agreement with the transport measurements for the four salts at room temperature.

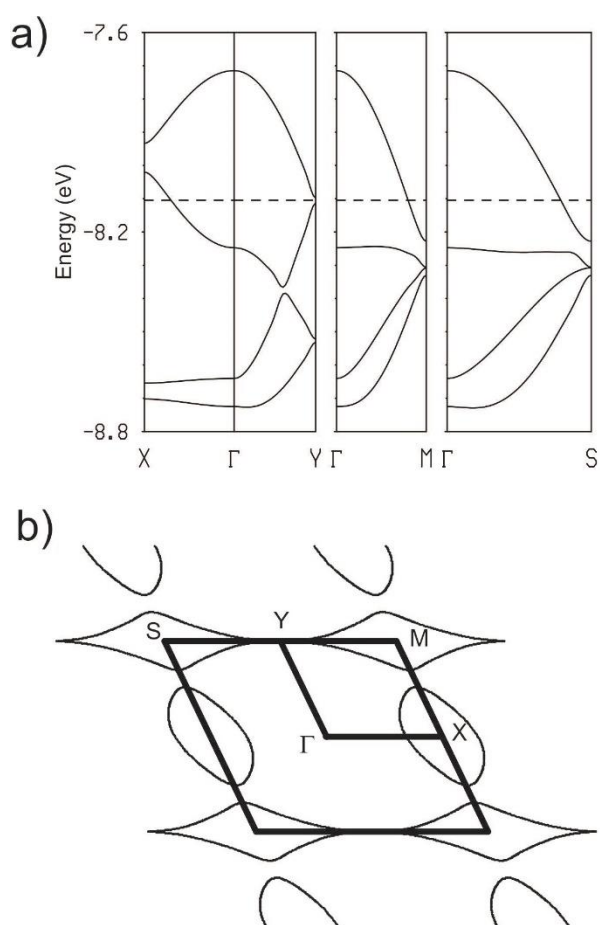


**Fig. 8** Calculated band structure (a) and Fermi surface (b) for the donor layers of  $\beta''$ -(BEDT-TTF)<sub>2</sub>[(H<sub>2</sub>O)(NH<sub>4</sub>)<sub>2</sub>Rh(C<sub>2</sub>O<sub>4</sub>)<sub>3</sub>]-18-crown-6 where  $\Gamma = (0, 0)$ ,  $X = (a^*/2, 0)$ ,  $Y = (0, b^*/2)$ ,  $M = (a^*/2, b^*/2)$  and  $S = (-a^*/2, b^*/2)$ .

The Fermi surfaces associated with the partially filled bands are reported in Figures 8b and 9b, respectively. Those for the **Cr** and **Ir** salts are reported in the Supplementary information (Figs. S1b and S2b, respectively). These Fermi surfaces, as it is the case for most  $\beta''$ -type salts,<sup>14</sup> result from the hybridization of a series of superposing ellipses with an area of 100% of the cross-section of the Brillouin zone. The Fermi surface of the **Rh** (Fig. 8b) and **Cr** (Fig. S1b) salts contain closed electron pockets around M (S) and hole pockets around X. The area of these pockets is ~11% of the cross-section of the Brillouin zone. The Fermi surfaces of the **Ru** (Fig. 9a) and **Ir** (Fig. S2b) are slightly different in that the pockets around M (S) communicate

through the Y point although the separation between the two lines around Y is so narrow that it is not clearly seen from the figures. The area of the closed pockets for these salts is  $\sim 13\%$  of the cross-section of the Brillouin zone. Note that the Fermi level cuts the upper band of Figs. 9a and S2a very near Y thus leading to the warped open line along the  $a^*$  direction. In contrast, the Fermi level is in the small gap at Y in Figs. 8a and S1a thus leading to closed pockets around M and S. The differences between the two series of Fermi surfaces could in principle be probed by magnetoresistance experiments. However, the differences are very small and should not be overemphasized. Magnetoresistance measurements need to be carried out at very low temperature and consequently, the thermal contraction below 110 K (the temperature of the crystal structure determination) may lead to structural variations and thus changes of the Fermi surface larger than those reported in our calculations.

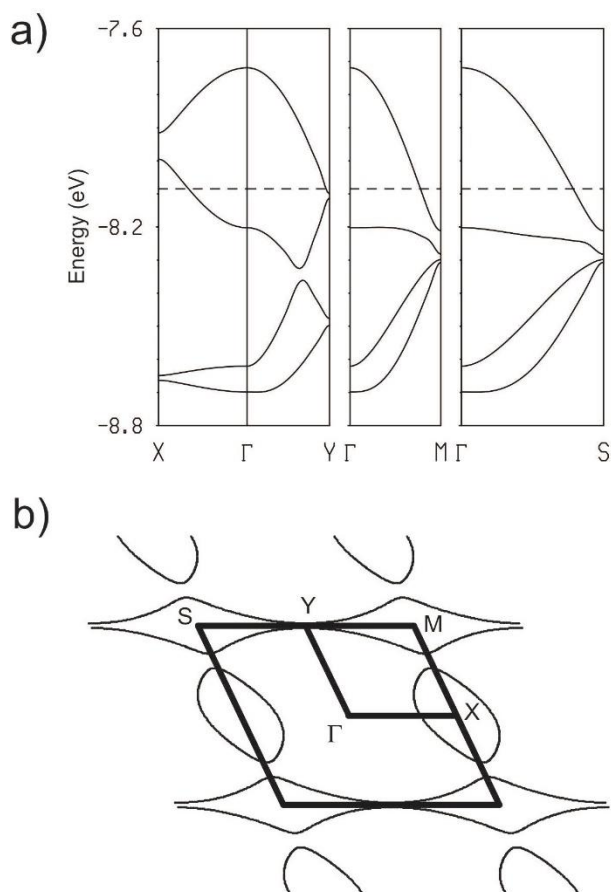


**Fig. 9** Calculated band structure (a) and Fermi surface (b) for the donor layers of  $\beta''$ -(BEDT-TTF) $_2$ [(H $_2$ O)(NH $_4$ ) $_2$ Ru(C $_2$ O $_4$ ) $_3$ ] $\cdot$ 18-crown-6 where  $\Gamma = (0, 0)$ ,  $X = (a^*/2, 0)$ ,  $Y = (0, b^*/2)$ ,  $M = (a^*/2, b^*/2)$  and  $S = (-a^*/2, b^*/2)$ .

The Fermi surfaces of the four salts do not exhibit nesting properties so that the metallic state should be preserved until low temperatures. This is certainly the case for the **Rh** and **Cr** salts but not for the **Ru** and **Ir** ones. Neither the nature of the HOMO $\cdots$ HOMO interactions nor the band structures and Fermi surfaces of the four salts exhibit any significant difference that could clearly justify the different behavior of the two pairs of salts. In addition, the metal-insulator transition of the **Ru** and **Ir** salts are very broad, clearly indicating that the transition must not have a structural origin mostly affecting the BEDT-TTF layers where the electron and hole carriers occur. The most likely reason for the broad metal-insulator transition is an electronic localization in the donor layers. We note that along the  $\cdots B \cdots A \cdots A \cdots B \cdots B \cdots A \cdots$  chains, interaction II (A $\cdots$ A) is very small and interaction I (B $\cdots$ B), although larger, is also clearly weaker than interaction III (A $\cdots$ B). In contrast, interactions along the step-chains and the lateral  $\pi$ -type interactions are more uniform. This may indicate a tendency towards electronic dimerization along the chains by locating the holes in the A $\cdots$ B pairs (*i.e.* a chain of Mott dimers). Disorder in the donor layers is often the origin of electronic localization in organic conductors. However, the degree of disorder in the present case is larger for the two salts not undergoing the metal-insulator transition (50:50 (Rh) and 59:41 (Cr) *versus* 70:30 (Ru) and 70:30 (Ir)). Thus, if our hypothesis is correct, the source of disorder must not be in the donor layers but in the region between these layers. As a matter of fact, structural transitions affecting mainly the anion layers have often been reported for different  $\beta''$ -(BEDT-TTF) $_4$ H $_3$ O[Fe(C $_2$ O $_4$ ) $_3$ ] $\cdot$ Guest salts where Guest is a solvent molecule.<sup>16,17</sup> We note that in the present salts there are



several quite short C-H...O contacts linking the BEDT-TTF donors and the anion layer so that structural changes in the anion layer could subtly be transmitted to the donor layers. In addition, the two salts undergoing the metal-insulator transition are associated with smaller interlayer *c* parameters than those keeping the metallic character suggesting that they are more constricted and their donor layers more sensitive to structural changes in the anion layers. Structural work as a function of temperature for the two series of salts will be performed to test our suggestion. However, there is another interesting possibility. All salts are isomorphous and therefore their anionic layers are very similar. The X-ray results indicate that their degrees of the disorder are not very different, which usually should not give any difference in interactions between cationic and anionic layers. Moreover, the Shubnikov–de Haas oscillation indicates that the electronic system is in a clean-limit. However, the subtle difference in the interlayer *c* axis (approximately 1% shorter) sometimes provides a large difference in physical properties, especially when the system is located on or near the border of some phases. We believe that the phase boundary is very different from a conventional one in the present case. We believe that the **Cr** and **Rh** salts do not show normal bulk superconductivity as observed in most organic conductors but instead show Berezinski-Kosterlitz–Thouless (BKT) superconductivity. This implies that the insulating ground states in the **Ir** and **Ru** salts could also have a BKT-like ground state, which is very different from previously reported ones that are observed in normal quasi-2D organic conductors. In the circumstance, the nature of the boundary, which may be between BKT superconductivity in the pure 2D system and a BKT-like ordering state in the quasi-2D system, should also be very different from conventional ones. However, we have no information about the details of the semiconducting state even though the slight change of the interlayer coupling may play an important role for the competition between the BKT superconductivity and the ordering states. Therefore, a better knowledge of the BKT superconducting state and other BKT states is needed. For researchers in the field of organic conductors, it is commonly accepted that the larger the counter-ion, the poorer the conductivity. The results reported here imply that, if BKT effects are important, pure 2D organic conductors have metallic or superconducting ground states. Research into BKT states in organic conductors is only just now starting. Work leading to the preparation and characterization of isomorphous salts may provide very useful hints on the nature of BKT states. This work is now in progress.

## EXPERIMENTAL DETAILS

**Rh, Cr:** reported previously<sup>11</sup>

**Ru, Ir:** ammonium tris(oxalato)metallate (200mg) was dissolved with the aid of 18-crown-6 (250mg) in acetophenone: 1,2,4-trichlorobenzene: ethanol (10:10:1ml) and filtered into the anode side of a two-compartment H-shaped electrochemical cell which contained BEDT-TTF (10mg).

After passing a current (1.0  $\mu$ A) through the solution for 21 days in dark and vibration-free conditions a large amount of black needle-shaped single crystals had grown and were collected with a scalpel.

Interlayer electrical resistivity measurements were performed on single crystals down to 1K using the AC four-probe method using carbon paint and  $\phi$ 10  $\mu$ m gold wires.

*Crystal data:* **Ru:** C<sub>38</sub>H<sub>50</sub>N<sub>2</sub>Ir<sub>1</sub>O<sub>19</sub>S<sub>16</sub>, *M* = 1452.85, black needle, *a* = 10.2959(2), *b* = 11.1722(3), *c* = 27.1422(5) Å,  $\alpha$  = 86.329(6),  $\beta$  = 82.859(6),  $\gamma$  = 64.347(5)°, *U* = 2792.35(15) Å<sup>3</sup>, *T* = 110 K, space group *P*-1, *Z* = 2,  $\mu$  = 0.951 mm<sup>-1</sup>, reflections collected = 27196, independent reflections = 12708, *R*1 = 0.0328, *wR*2 = 0.0813 [*F*<sup>2</sup> > 2 $\sigma$ (*F*<sup>2</sup>)], *R*1 = 0.0408, *wR*2 = 0.0847 (all data).

*Crystal data:* **Ir:** C<sub>38</sub>H<sub>50</sub>N<sub>2</sub>Ir<sub>1</sub>O<sub>19</sub>S<sub>16</sub>, *M* = 1544.00, black needle, *a* = 10.3115(3), *b* = 11.1855(4), *c* = 27.1250(7) Å,  $\alpha$  = 86.213(6),  $\beta$  = 82.827(6),  $\gamma$  = 64.215(5)°, *U* = 2794.78(18) Å<sup>3</sup>, *T* = 110 K, space group *P*-1, *Z* = 2,  $\mu$  = 3.065 mm<sup>-1</sup>, reflections collected = 26988, independent reflections = 12712, *R*1 = 0.0465, *wR*2 = 0.1033 [*F*<sup>2</sup> > 2 $\sigma$ (*F*<sup>2</sup>)], *R*1 = 0.0634, *wR*2 = 0.1089 (all data).

CCDC 1892600 and 1892602 contains supplementary X-ray crystallographic data for **Ru** and **Ir**, respectively. This data can be obtained free of charge via <http://www.ccdc.cam.ac.uk/conts/retrieving.html>, or from the Cambridge Crystallographic Data Centre, Union Road, Cambridge, CB2 1EZ; fax(+44) 1223-336-033 or email: [deposit@ccdc.cam.ac.uk](mailto:deposit@ccdc.cam.ac.uk).

## COMPUTATIONAL DETAILS

The tight-binding band structure calculations<sup>19</sup> were of the extended Hückel type. A modified Wolfsberg-Helmholtz formula was used to calculate the non-diagonal *H* <sub>$\mu\nu$</sub>  values.<sup>20</sup> All valence electrons were taken into account in the calculations and the basis set consisted of Slater-type orbitals of double- $\zeta$  quality for C 2s and 2p, S 3s and 3p and of single- $\zeta$  quality for H 1s.

The ionization potentials, contraction coefficients and exponents were taken from previous work.<sup>21</sup>

## CONCLUSIONS

The series of salts  $\beta''$ -(BEDT-TTF)<sub>2</sub>[(H<sub>2</sub>O)(NH<sub>4</sub>)<sub>2</sub>M(C<sub>2</sub>O<sub>4</sub>)<sub>3</sub>].18-crown-6 show ambient-pressure superconductivity when *M* = Cr or Rh<sup>11</sup> and evidence indicates that they show a bulk Berezinski-Kosterlitz-Thouless superconducting transition.<sup>12</sup> The distance between neighbouring conducting layers is the widest found in a radical-cation salt having just the one BEDT-TTF packing type ( $\beta''$ ). The isostructural ruthenium and iridium salts are reported here for the first time.

The iridium salt represents the first radical-cation salt to contain a 5d tris(oxalato)metallate anion. Both of these salts do not show superconductivity but instead undergo a broad chemically-induced metal-to-insulator transition at 155 K for ruthenium and at 100 K for iridium. The *c* axes of the Ru and Ir salts are much shorter than those of the Rh and Cr salts. Since the direction of the *c* axis corresponds to the interlayer direction, the difference of the electronic states is expected to originate from dimensionality, *i.e.* interlayer interaction. The two superconducting salts should have better two-dimensionality compared with the two metal-insulator salts. Very small differences in the Fermi surfaces are observed between the Rh and Cr salts versus the Ru and Ir salts. The metal-insulator transition of the Ru and Ir salts may originate from changes in the anionic layers which are more easily transmitted to the conducting layers for these more constricted salts. However it can also originate from BKT effects.

We are continuing our studies on this  $\beta''$ -(BEDT-TTF)<sub>2</sub>[(H<sub>2</sub>O)(NH<sub>4</sub>)<sub>2</sub>M(C<sub>2</sub>O<sub>4</sub>)<sub>3</sub>].18-crown-6 family by synthesising new salts with other metal centres or crown ethers. We are also performing resistivity measurements under pressure on the Cr salt, and using chemical pressure by doping Cr with Ir to produce salts with intermediate *c* axis lengths, to explore the transition from superconductor to semiconductor.

## SUPPORTING INFORMATION

Calculated band structure and Fermi surface for the donor layers of **Cr** and **Ir**.

## ACKNOWLEDGEMENT

LM would like to thank the Royal Society and Leverhulme Trust for a Senior Research Fellowship. JRL and LM would like to thank Nottingham Trent University for PhD funding. E.C. acknowledges support by MINECO (Spain) through Grant FIS2015-64886-C5-4-P and the Severo Ochoa Centers of Excellence Program (Grant SEV-2015-0496) as well as by Generalitat de Catalunya (2014SGR301).

## AUTHOR INFORMATION

Corresponding Author

Email: [lee.martin@ntu.ac.uk](mailto:lee.martin@ntu.ac.uk)

Author Contributions

The manuscript was written through contributions of all authors.

Funding Sources

This work has been supported by a Royal Society Leverhulme Trust Senior Research Fellowship, a JSPS [KAKENHI Grant Number JP17H01144] and Royal Society [Research Grants (RG100853 and RG081209), International Exchange Scheme (IE130367 and IE150152), and International Joint Project (JP0869972)].

Notes

The authors declare no competing financial interests.

## REFERENCES

- 1 Martin, L. Molecular conductors of BEDT-TTF with tris(oxalato)metallate anions, *Coord. Chem. Rev.*, **2018**, *376*, 277-291.
- 2 Kurmoo, M.; Graham, A. W.; Day, P.; Coles, S. J.; Hursthouse, M. B.; Caulfield, J. L.; Singleton, J.; Pratt, F. L.; Hayes, W.; Ducasse, L.; Guionneau, P. Superconducting and Semiconducting Magnetic Charge Transfer Salts: (BEDT-TTF)<sub>4</sub>AFe(C<sub>2</sub>O<sub>4</sub>)<sub>3</sub>·C<sub>6</sub>H<sub>5</sub>CN (A = H<sub>2</sub>O, K, NH<sub>4</sub>), *J. Am. Chem. Soc.*, **1995**, *117*, 12209.
- 3 Coronado, E.; Galán-Mascarós, J. R.; Gómez-García, C. J.; Laukhin, V. Coexistence of ferromagnetism and metallic conductivity in a molecule-based layered compound, *Nature*, **2000**, *408*, 447.
- 4 Zhang, B.; Zhang, Y.; Zhu, D. (BEDT-TTF)<sub>3</sub>Cu<sub>2</sub>(C<sub>2</sub>O<sub>4</sub>)<sub>3</sub>(CH<sub>3</sub>OH)<sub>2</sub>: an organic-inorganic hybrid antiferromagnetic semiconductor, *Chem. Commun.*, **2012**, *48*, 198-199.
- 5 Martin, L.; Day, P.; Horton, P. N.; Nakatsuji, S.-i.; Yamada, J.-i.; Akutsu, H. Chiral conducting salts of BEDT-TTF containing a single enantiomer of tris(oxalato)chromate(III) crystallised from a chiral solvent, *J. Mater. Chem.*, **2010**, *20*, 2738-2742; Martin, L.; Day, P.; Nakatsuji, S.-i.; Yamada, J.-i.; Akutsu, H.; Horton, P. N. A molecular charge transfer salt of BEDT-TTF containing a single enantiomer of tris(oxalato)chromate(III) crystallised from a chiral solvent, *CrystEngComm*, **2010**, *12*, 1369-1372; Martin, L.; Engelkamp, H.; Akutsu, H.; Nakatsuji, S.-i.; Yamada, J.-i.; Horton, P. N.; Hursthouse, M. B. Radical-cation salts of BEDT-TTF with lithium tris(oxalato)metallate(III), *Dalton Trans.*, **2015**, *44*, 6219-6223; Martin, L.; Akutsu, H.; Horton, P. N.; Hursthouse, M. B. Chirality in charge-transfer salts of BEDT-TTF of tris(oxalato)chromate(III), *CrystEngComm*, **2015**, *17*, 2783-2790; Martin, L.; Akutsu, H.; Horton, P. N.; Hursthouse, M. B.; Harrington, R. W.; Clegg, W. Chiral Radical-Cation Salts of BEDT-TTF Containing a Single Enantiomer of Tris(oxalato)aluminate(III) and -chromate(III), *Eur. J. Inorg. Chem.*, **2015**, 1865-1870.

6 Turner, S. S.; Day, P.; Malik, K. M. A.; Hursthouse, M. B.; Teat, S. J.; MacLean, E. J.; Martin, L.; French, S. A. Effect of included solvent molecules on the physical properties of the paramagnetic charge transfer salts  $\beta''$ -[bedt-ttf]<sub>4</sub>[(H<sub>3</sub>O)Fe(C<sub>2</sub>O<sub>4</sub>)<sub>3</sub>]-solvent (bedt-ttf = bis(ethylenedithio)tetrathiafulvalene), *Inorg. Chem.*, **1999**, *38*, 3543–3549; Rashid, S.; Turner, S. S.; Day, P.; Howard, J. A. K.; Guionneau, P.; McInnes, E. J. L.; Mabbs, F. E.; Clark, R. J. H.; Firth, S.; Biggs, T. New superconducting charge-transfer salts (BEDT-TTF)<sub>4</sub>[A·M(C<sub>2</sub>O<sub>4</sub>)<sub>3</sub>]-C<sub>6</sub>H<sub>5</sub>NO<sub>2</sub> (A = H<sub>3</sub>O or NH<sub>4</sub>, M = Cr or Fe, BEDT-TTF = bis(ethylenedithio)tetrathiafulvalene), *J. Mater. Chem.*, **2001**, *11*, 2095–2101; Coronado, E.; Curreli, S.; Giménez-Saiz, C.; Gómez-García, C. J. The Series of Molecular Conductors and Superconductors ET<sub>4</sub>[AFe(C<sub>2</sub>O<sub>4</sub>)<sub>3</sub>]-PhX (ET = bis(ethylenedithio)tetrathiafulvalene; (C<sub>2</sub>O<sub>4</sub>)<sup>2-</sup> = oxalate; A<sup>+</sup> = H<sub>3</sub>O<sup>+</sup>, K<sup>+</sup>; X = F, Cl, Br, and I): Influence of the Halobenzene Guest Molecules on the Crystal Structure and Superconducting Properties, *Inorg. Chem.*, **2012**, *51*, 1111–1126.

7 Akutsu, H.; Akutsu-Sato, A.; Turner, S. S.; Day, P.; Canadell, E.; Firth, S.; Clark, R. J. H.; Yamada, J.-i.; Nakatsuji, S.-i. Superstructures of donor packing arrangements in a series of molecular charge transfer salts, *Chem. Commun.*, **2004**, 18–19; Martin, L.; Day, P.; Akutsu, H.; Yamada, J.-i.; Nakatsuji, S.-i.; Clegg, W.; Harrington, R. W.; Horton, P. N.; Hursthouse, M. B.; McMillan, P.; Firth, S. Metallic molecular crystals containing chiral or racemic guest molecules, *CrystEngComm*, **2007**, *9*, 865–867.

8 Zorina, L. V.; Khasanov, S. S.; Simonov, S. V.; Shibaeva, R. P.; Zverev, V. N.; Canadell, E.; Prokhorova, T. G.; Yagubskii, E. B. Coexistence of two donor packing motifs in the stable molecular metal  $\alpha$ -pseudo- $\kappa$ -(BEDT-TTF)<sub>4</sub>(H<sub>3</sub>O)[Fe(C<sub>2</sub>O<sub>4</sub>)<sub>3</sub>]-C<sub>6</sub>H<sub>4</sub>Br<sub>2</sub>, *CrystEngComm*, **2011**, *13*, 2430–2438; Prokhorova, T. G.; Buravov, L. I.; Yagubskii, E. B.; Zorina, L. V.; Simonov, S. V.; Shibaeva, R. P.; Zverev, V. N. Metallic Bi- and Monolayered Radical Cation Salts Based on Bis(ethylenedithio)tetrathiafulvalene (BEDT-TTF) with the Tris(oxalato)gallate Anion, *Eur. J. Inorg. Chem.*, **2014**, 3933–3940;

9 Martin, L.; Day, P.; Clegg, W.; Harrington, R. W.; Horton, P. N.; Bingham, A.; Hursthouse, M. B.; McMillan, P.; Firth, S. Multi-layered molecular charge-transfer salts containing alkali metal ions, *J. Mater. Chem.*, **2007**, *17*, 3324–3329.

10 Rashid, S.; Turner, S. S.; Day, P.; Light, M. E.; Hursthouse, M. B.; Firth, S.; Clark, R. J. H. The first molecular charge transfer salt containing proton channels, *Chem. Commun.*, **2001**, 1462–1463; Akutsu-Sato, A.; Akutsu, H.; Turner, S. S.; Day, P.; Probert, M. R.; Howard, J. A. K.; Akutagawa, T.; Takeda, S.; Nakamura, T.; Mori, T. The First Proton-Conducting Metallic Ion-Radical Salts, *Angew.Chem.Ind.Ed.*, **2005**, *44*, 291.

11 Martin, L.; Morrirt, A. L.; Lopez, J. R.; Akutsu, H.; Nakazawa, Y.; Imajo, S.; Ihara, Y. Ambient-pressure molecular superconductor with a superlattice containing layers of tris(oxalato)rhodate enantiomers and 18-crown-6, *Inorg. Chem.*, **2017**, *56*, 717–720; Martin, L.; Morrirt, A. L.; Lopez, J. R.; Akutsu, H.; Nakazawa, Y.; Imajo, S. Quasi-Kosterlitz-Thouless molecular superconductor  $\beta''$ -(BEDT-TTF)<sub>2</sub>[(H<sub>2</sub>O)(NH<sub>4</sub>)<sub>2</sub>Cr(C<sub>2</sub>O<sub>4</sub>)<sub>3</sub>].18-crown-6, *Inorg. Chem.*, **2017**, *56*, 14045–14052.

12 Kosterlitz, J. M.; Thouless, D. J. Long range order and metastability in two dimensional solids and superfluids. (Application of dislocation theory), *J. Phys. C: Solid State Phys.*, **1972**, *5*, L124; Kosterlitz, J. M.; Thouless, D. J. Ordering, metastability and phase transitions in two-dimensional systems, *J. Phys. C: Solid State Phys.*, **1973**, *6*, 1181; Kosterlitz, J. M. The critical properties of the two-dimensional xy model, *J. Phys. C: Solid State Phys.*, **1974**, *7*, 1046; Berezinski, V. L. Destruction of Long-range Order in One-dimensional and Two-dimensional Systems having a Continuous Symmetry Group I. Classical Systems, *Sov. Phys. J. Exper. Theor. Phys.*, **1971**, *32*, 493; Advanced information. NobelPrize.org. Nobel Media AB 2018. Thu. 20 Dec 2018. <https://www.nobelprize.org/prizes/physics/2016/advanced-information/>

13 Guionneau, P.; Kepert, C. J.; Chasseau, D.; Truter, M.R.; Day, P. Determining the charge distribution in BEDT-TTF Salts, *Synth. Met.*, **1997**, *86*, 1973.

14 Rousseau, R.; Gener, M.; Canadell, E. Step-by-Step Construction of the Electronic Structure of Molecular Conductors: Conceptual Aspects and Application, *Adv. Funct. Mat.*, **2004**, *14*, 201–214.

15 Whangbo, M.-H.; Williams, J. M.; Leung, P. C. W.; Beno, M. A.; Emge, T. J.; Wang, H. H. Role of the Intermolecular Interactions in the Two-Dimensional Ambient-Pressure Organic Superconductors  $\beta$ -(ET)<sub>2</sub>I<sub>3</sub> and  $\beta$ -(ET)<sub>2</sub>IBr<sub>2</sub>, *Inorg. Chem.*, **1985**, *24*, 3500–3502.

16 Zorina, L. V.; Khasanov, S. S.; Simonov, S. V.; Shibaeva, R. P.; Bulanchuk, P. O.; Zverev, V. N.; Canadell, E.; Prokhorova, T. G.; Yagubskii, E. B. Structural phase transition in the  $\beta''$ -(BEDT-TTF)<sub>4</sub>H<sub>3</sub>O[Fe(C<sub>2</sub>O<sub>4</sub>)<sub>3</sub>]-G crystals (where G is a guest solvent molecule), *CrystEngComm*, **2012**, *14*, 460–465.

17 Prokhorova, T. G.; Buravov, L. I.; Yagubskii, E. B.; Zorina, L. V.; Simonov, S. V.; Zverev, V. N.; Shibaeva, R. P.; Canadell, E. Effect of Halopyridine Guest Molecules on the Structure and Superconducting Properties of  $\beta''$ -(BEDT-TTF)<sub>4</sub>(H<sub>3</sub>O)[Fe(C<sub>2</sub>O<sub>4</sub>)<sub>3</sub>]-Guest Crystals, *Eur. J. Inorg. Chem.*, **2015**, 5611–5620.

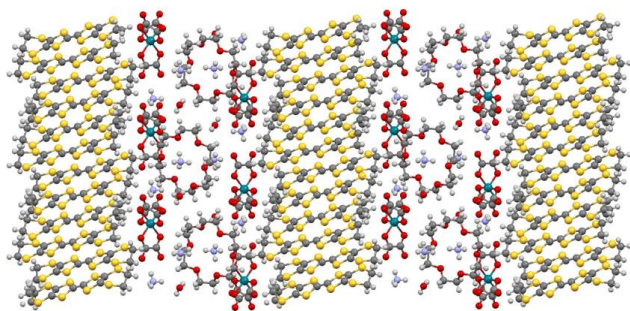
18 Prokhorova, T. G.; Zorina, L. V.; Simonov, S. V.; Zverev, V. N.; Canadell, E.; Shibaeva, R. P.; Yagubskii, E. B. The first molecular superconductor based on BEDT-TTF radical cation salt with paramagnetic tris(oxalato)ruthenate anion, *CrystEngComm*, **2013**, *15*, 7048–7055.

19 Whangbo, M.-H.; Hoffmann, R. The Band Structure of the Tetracyanoplatinate Chain, *J. Am. Chem. Soc.*, **1978**, *100*, 6093–6098.

20 Ammeter, J. H.; Bürgi, H.-B.; Thibeault, J.; Hoffmann, R. Counterintuitive mixing in semiempirical and ab initio molecular orbital calculations, *J. Am. Chem. Soc.*, **1978**, *100*, 3686–3692.

21 Pénicaud, A.; Boubekour, K.; Batail, P.; Canadell, E.; Auban-Senzier, P.; Jérôme, D. Hydrogen-bond tuning of macroscopic transport properties from the neutral molecular component site along the series of metallic organic-inorganic solvates (BEDT-TTF)<sub>4</sub>Re<sub>6</sub>Se<sub>5</sub>Cl<sub>9</sub>·[guest], [guest = DMF, THF, dioxane], *J. Am. Chem. Soc.*, **1993**, *115*, 4101-4112.

## SYNOPSIS TOC



The series of salts  $\beta''$ -(BEDT-TTF)<sub>2</sub>[(H<sub>2</sub>O)(NH<sub>4</sub>)<sub>2</sub>M(C<sub>2</sub>O<sub>4</sub>)<sub>3</sub>].18-crown-6 show ambient-pressure superconductivity when M = Cr or Rh. Evidence indicates that both salts show a bulk Berezinski-Kosterlitz-Thouless superconducting transition. This paper reports the isostructural ruthenium and iridium salts. Both the Ru and Ir salts do not show superconductivity but instead undergo a metal-insulator transition at 155 K for ruthenium and at 100 K for iridium.

---